Decadal Variability of Precipitation over Western North America

DANIEL R. CAYAN

Climate Research Division, Scripps Institution of Oceanography, and Water Resources Division, U.S. Geological Survey, La Jolla, California

MICHAEL D. DETTINGER

Water Resources Division, U.S. Geological Survey, Scripps Institution of Oceanography, La Jolla, California

HENRY F. DIAZ

NOAA/ERL/CDC, Boulder, Colorado

NICHOLAS E. GRAHAM

Climate Research Division, Scripps Institution of Oceanography, La Jolla, California

(Manuscript received 6 January 1997, in final form 27 May 1998)

ABSTRACT

Decadal (>7- yr period) variations of precipitation over western North America account for 20%–50% of the variance of annual precipitation. Spatially, the decadal variability is broken into several regional [*O*(1000 km)] components. These decadal variations are contributed by fluctuations in precipitation from seasons of the year that vary from region to region and that are not necessarily concentrated in the wettest season(s) alone. The precipitation variations are linked to various decadal atmospheric circulation and SST anomaly patterns where scales range from regional to global scales and that emphasize tropical or extratropical connections, depending upon which precipitation region is considered. Further, wet or dry decades are associated with changes in frequency of at least a few short-period circulation ''modes'' such as the Pacific–North American pattern. Precipitation fluctuations over the southwestern United States and the Saskatchewan region of western Canada are associated with extensive shifts of sea level pressure and SST anomalies, suggesting that they are components of low-frequency precipitation variability from global-scale climate processes. Consistent with the global scale of its pressure and SST connection, the Southwest decadal precipitation is aligned with opposing precipitation fluctuations in northern Africa.

1. Introduction

Understanding the nature and causes of decadal fluctuations in precipitation is an unresolved problem, partly because observed records are relatively short or sparse and because dynamical processes that operate on this timescale are not firmly identified. Much attention has been devoted to how and why precipitation varies in association with the El Niño–Southern Oscillation (ENSO) (Ropelewski and Halpert 1986; Diaz and Kiladis 1992; Redmond and Koch 1991). However, decadal-scale fluctuations are crucial because they control water supplies, affect biota, and may modulate higher-frequency events such as floods and drought. Also, low-frequency natural variability is an important factor in global change issues because it may obscure human influences on hydrologic variations. The western part of North America should be suited to a study of these long-term fluctuations because of its proximity to the Pacific Ocean, which is noted as a seat of low-frequency climate variability (Douglas et al. 1982; Trenberth 1990; Latif and Barnett 1994; Mantua et al. 1997). Furthermore, much of western North America is dominated by winter precipitation from North Pacific storms (Pyke 1972). Accordingly, the domain of the present study covers midlatitude North America from the Pacific coast to the eastern side of the Rocky Mountains.

Examples of multiyear hydroclimatic events in the western North America region during the instrumental period include the recent (1987–92) California drought (e.g., Roos 1994), slow changes in western streamflow

Corresponding author address: Dr. Daniel R. Cayan, Climate Research Division, Scripps Institution of Oceanography, La Jolla, CA 92093-0224.
E-mail: dcayan@ucsd.edu

patterns (Langbein and Slack 1982), changes in snowpack across the Rocky Mountains (Changnon et al. 1993), trends in the timing of runoff from the Sierra Nevada and other mountainous regions of the western United States (Roos 1991; Aguado et al. 1992; Wahl 1992; Dettinger and Cayan 1995), and multidecadal groundwater fluctuations (Dettinger and Schaefer 1995). Webb and Betancourt (1990) documented changes in flood frequency in southern Arizona associated with multidecade climate variability, and Ely et al. (1994) identified multiyear swings in the frequency of large floods in several rivers in the Southwest from available historical records. Additional evidence for long wet and dry spells is provided by proxy recorders of the recent paleoclimate of this region (Hughes and Brown 1992; Meko et al. 1993; Stine 1994; Stahle and Cleveland 1988).

What is not clear is the extent to which long-lived wet and dry spells are organized across western North America. Is there spatial structure that recurs from episode to episode? A complication is that precipitation is strongly seasonal, so that in most of this region the wet season of each year is interrupted by a dry season, which could potentially ''clean the slate'' for the following wet season. Thus, it is also not clear whether certain slowly changing climate elements can be identified that provide a memory that produces spells of anomalous precipitation. Alternatively, it might be that these spells are the low-frequency residual of random processes, that is, nothing more than reddened noise. To approach these questions, this paper and a companion study of zonally averaged precipitation along the North American west coast by Dettinger et al. (1998) describe aspects of interannual–decadal-scale variability. Here we examine the following aspects of decadal precipitation variability (periods of 7 yr and greater) over western North America: 1) What is the spatial structure of decadal precipitation fluctuations over the West from the Rocky Mountains to the Pacific coast? 2) How are regional decadal precipitation anomalies related to atmospheric circulation and sea surface temperatures?

2. Data

The primary data are a global gridded (5° lat × 5° long) monthly set of precipitation anomaly time series (Eischeid et al. 1991; Eischeid et al. 1995). These data consist of area averages of monthly anomalies from individual cooperative and first-order stations. For our effort, we focus on grid points with adequate data history (at least 45 yr). Monthly anomalies for all stations within each 5° grid box were weighted by an inverse-distance procedure to yield the anomalous precipitation, centered at each grid point. Analyses herein are restricted to the time period after 1880 because earlier data are relatively sparse, and the precipitation data end in 1994. For most of the present study, the spatial domain of precipitation data for most of the present study is western North America from 100°W westward to the Pacific coast, and from 30° to 60°N (Fig. 1), although we later consider precipitation anomalies over all available global land areas for comparative purposes.

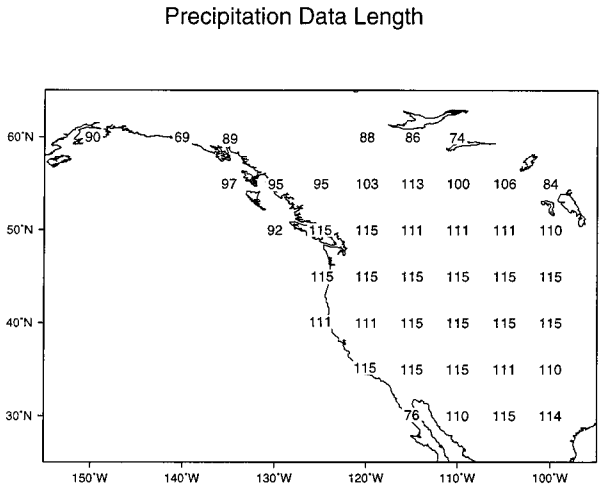

FIG. 1. Precipitation grid, showing number of years of observations.

Historical precipitation data contain a number of observational inaccuracies (Groisman and Legates 1994) and these may affect some of the apparent variability at low frequencies. Also, in the complex terrain of much of the West, most weather stations are located in lower elevations (e.g., valleys), so there is a low-elevation bias in the precipitation observation network. However, the regional patterns investigated herein are shown to be loosely consistent with independent records of snowpack and streamflow, so these problems probably are not severe.

Streamflow is from selected U.S. and Canadian stream gauges (United States Geological Survey and other sources) having relatively long periods (as early as 1890 to the present; see Cayan and Peterson 1989). Streamflow is a useful climate measure because it represents runoff over a broad region and generally represents a time period of a few months. Snow accumulation is from a set of 1 April snow course observations in selected regions (Changnon et al. 1993; Cayan 1996) with records generally beginning as early as the 1910s. Snowpack is the accumulation of snow water over the winter—1 April is typically the zenith of snow accumulation and thus provides a measurement of the high-elevation precipitation for the entire winter.

Gridded sea level pressure (SLP) anomalies are used to diagnose the atmospheric circulation patterns associated with low-frequency precipitation fluctuations. SLP anomalies (from 1951–92 monthly means) on a 5° lat × 5° long grid from 42.5°S to 72.5°N were obtained from the Scripps Institution of Oceanography, which developed the set from the U.S. National Meteorological Center, the U.S. Navy Fleet Numerical Oceanography Center (Monterey, California), and the Australian, New

Zealand, and South African meteorological bureaus (Barnett et al. 1984).

Sea surface temperature (SST) data employed are 1880–1991 monthly averages on a 5° lat × 5° long global grid from the GISST adjusted-anomaly set provided by the Hadley Centre (Parker et al. 1995). Anomalies were adjusted by the authors of the dataset in an attempt to remove artificial biases and changes in the series arising from changes in instrumental techniques. A significant amount of missing data was filled-in by the GISST dataset authors by using several EOFs constructed from the more recent, better sampled period of the SST record, based upon remote-sensed (IR radiometer) SST as well as from conventional ship data. In so doing, some of the finer spatial-scale SST structure has been filtered out, but this is of minor importance for our purposes.

3. Decadal patterns of precipitation variability

a. Fraction of variability in decadal frequencies

The precipitation and many of the ancillary data were low-pass filtered to form decadal anomalies as well as bandpass filtered to form ENSO-band anomalies. The filter employed is a Kaylor filter (Kaylor 1977) with half-power points at 36 months and 84 months for the ENSO band-passed components, and a half-power point at 84 months for the decadal low-passed components. Precipitation variability contained in the low-frequency band is substantial (Fig. 2). The decadal band contains more than 30% of the total annual variance at most grid points (lower panel of Fig. 2), and the ENSO band contributes more than 20% (middle panel of Fig. 2). In particular, decadal fluctuations account for greater than 50% of the total variability in the southern and northern part of the domain, while ENSO fluctuations account for a relatively large portion of total variability over the Pacific Northwest. Some of the low-passed precipitation variability is actually ultra-low-frequency change (i.e., trends, etc.), but a similar calculation using bandpass filtering to isolate periods between 7 and 40 yr, showed that contributions by ''trends'' are not too strong. Thus, decadal components are, in this sense, of comparable importance to the more studied ENSO-scale variability.

b. Regional precipitation patterns

Inspection of various hydrologic records over western North America indicates that there is considerable inhomogeneity over the region (Sellers 1968). The time series of the domain average of the decadal precipitation has maximum correlation of 0.5 to the decadal precipitation series at any one grid point, and most are less than 0.3. To extract coherent packets of variability, principal components (PCs) were calculated using the 42 grid points having at least 80 yr of data (Fig. 1). Then, the leading PCs were recombined using a varimax rotation (Richman 1986). The rotated PCs (RPCs) have relatively broad, strong expressions—these are used to represent the regional decadal modes that are the focus of several subsequent analyses. The varimax rotation may yield more physically realistic patterns than the original patterns because it produces more regionally clustered spatial loadings, maximizing the variance of the squared correlation between the RPCs and the original time series (Horel 1981; Richman 1986; Barnston and Livezey 1987, hereafter BL). Under this rotation, the orthogonality of the time coefficients (RPCs) is preserved, but the spatial loading maps are not necessarily orthogonal. In this case, six EOFs were rotated; spatial weights of these six RPCs are shown in Fig. 3. These six leading modes explain 68% of the precipitation field variance in the decadal ''band'' over the study region.

Experimentation showed that the resulting RPCs are not very sensitive to the choice of grid domain or to the number of EOFs included in the rotation. A broader grid, a shorter time series (1900–94), and more EOFs rotated (as many as 12) produced leading modes with very similar spatial and temporal structure. The spatial loading patterns associated with each RPC have regional centers over the southwestern United States, the Pacific Northwest, California–Nevada, the Canadian prairies, Alaska and northwestern Canada, and the central-northern Rockies, respectively. Hereafter these RPCs and their spatial patterns are called Southwest, Northwest, California, Saskatchewan, Far North, and Wyoming. Most of the RPC loadings contain a regional center with scale of about 1000 km, where a sizable fraction (50% or more) of the decadal precipitation variance is explained. Three of the patterns (Southwest, Saskatchewan, and California) also contain weak out-of-phase variability over remote locations. While these are too flimsy to warrant much attention here, it is worth noting that there is a tendency for the precipitation supply to be redistributed, producing opposing anomalies between southern and northern latitudes. Tendencies for opposing north–south precipitation anomalies along the West Coast are analyzed in greater detail by Dettinger et al. (1998).

The decadal variability captured by the regional precipitation RPC series may be compared with that of other independently observed measures of the surface hydrology. To this end, time series of decadal filtered 1 April snow accumulation and annual streamflow from selected snow courses and stream gauges within the regional centers of the RPC loading patterns are plotted together with their corresponding RPCs in Fig. 4. Snow course data were not available for the Saskatchewan and Far North regions. The decadal fluctuations of snow accumulation and streamflow are quite consistent with those for each region's precipitation, although there may be discrepancies because snow accumulation and streamflow have such a strong winter character.

The RPCs and associated streamflow and snow accumulation series exhibit prominent multiyear anoma-

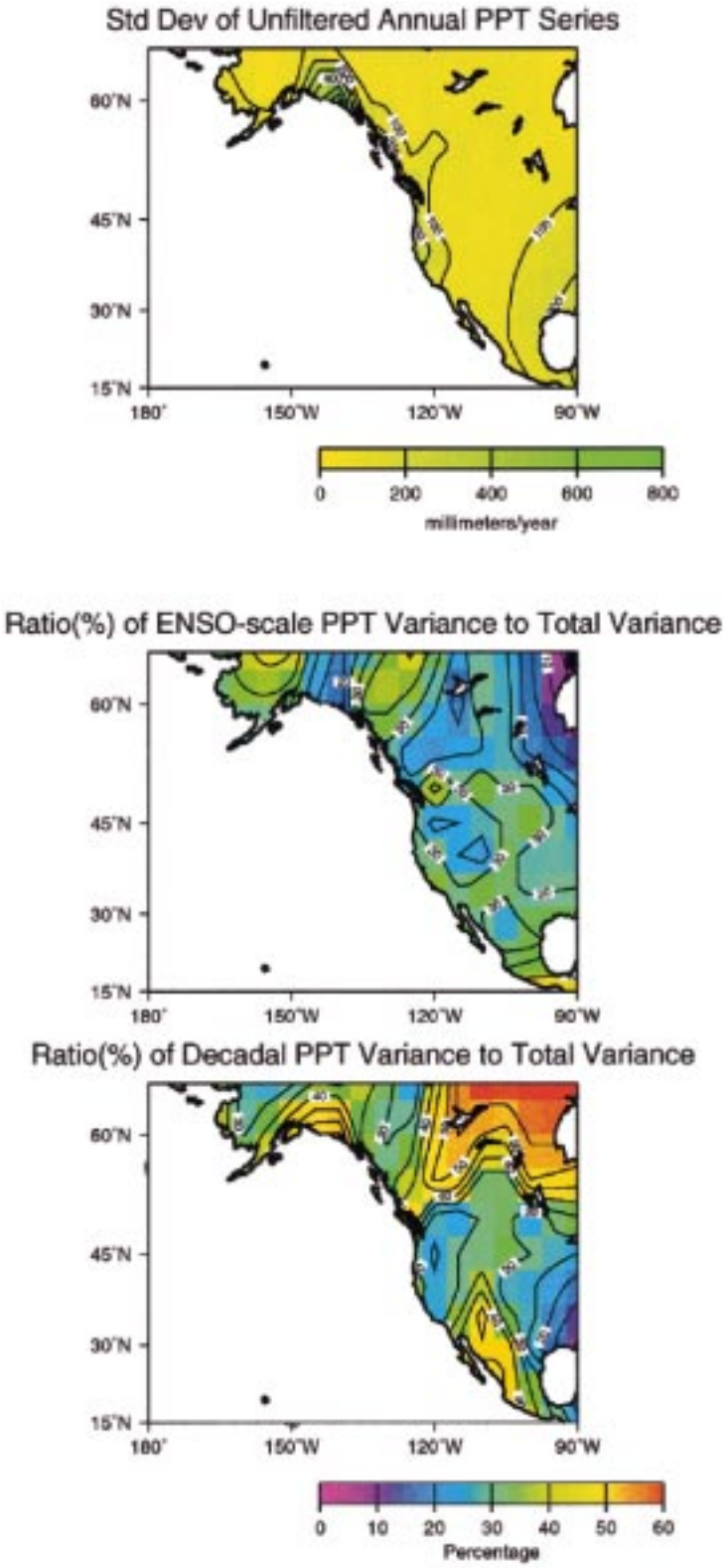

FIG. 2. Standard deviation (mm) of (top) annual precipitation and (middle) fraction of variance explained by ENSO and (bottom) decadal frequency bands.

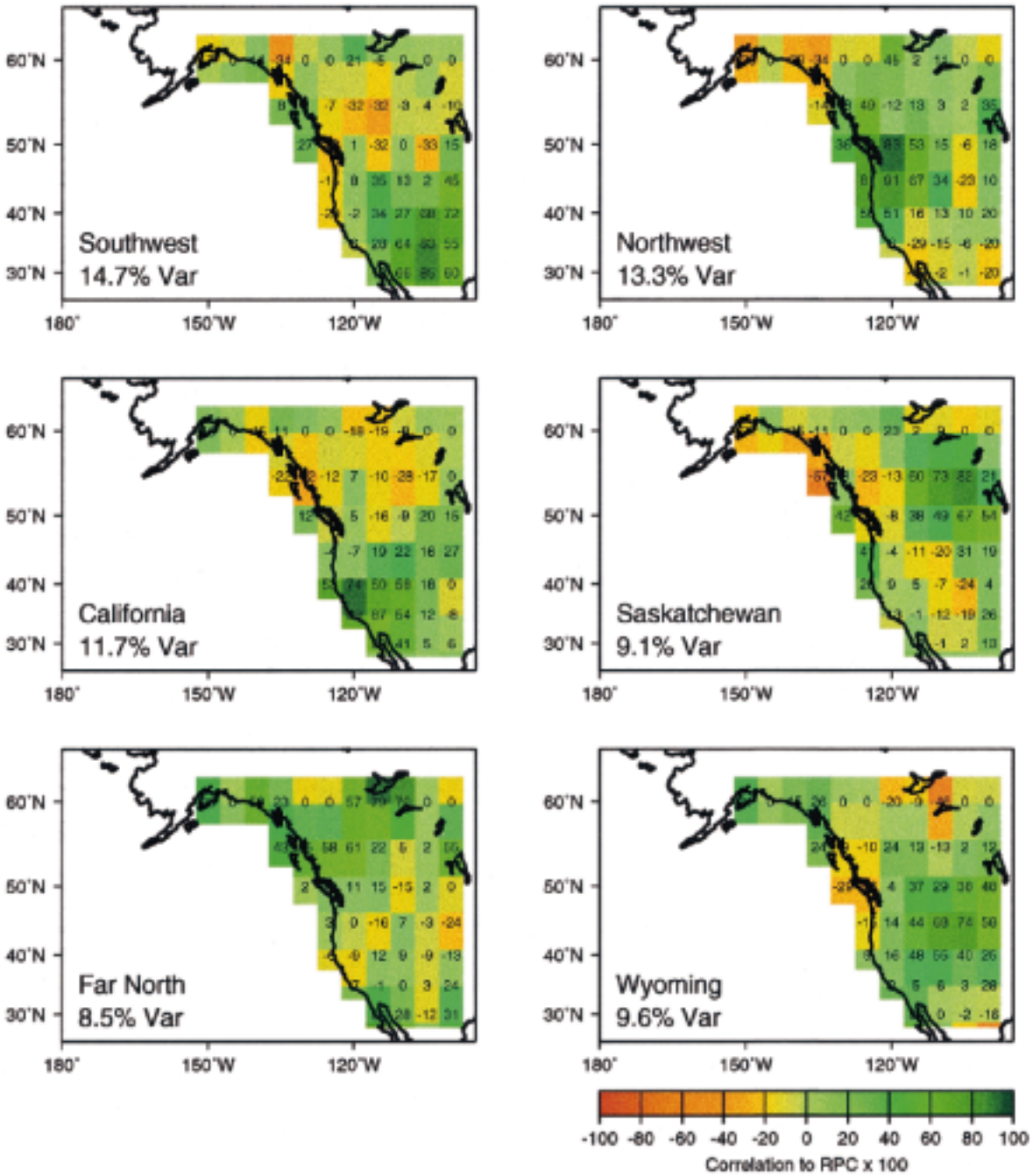

FIG. 3. Spatial loadings for first six RPCs of decadal precipitation. These are expressed as correlations between the RPCs and the original decadal precipitation time series at each grid point.

lies for the respective regions. Especially notable are the transition from generally dry to generally wet around 1950 in the Northwest, long midcentury dry spells in Wyoming, and dry episodes in California that are spaced at fairly regular intervals of 15 yr apart. Some important features during the early part of the record (e.g., mid- to late 1800s through early 1900s) are indicated by scattered observations, but are not well resolved. This includes the apparent very high precipitation in the Southwest during the 1880s (Fig. 4); this episode is supported by observations that many of the present-day arroyos in the Southwest were cut during this episode (Webb et al. 1991). Together the series in Fig. 4 demonstrate that the precipitation patterns identified by this RPC pro-

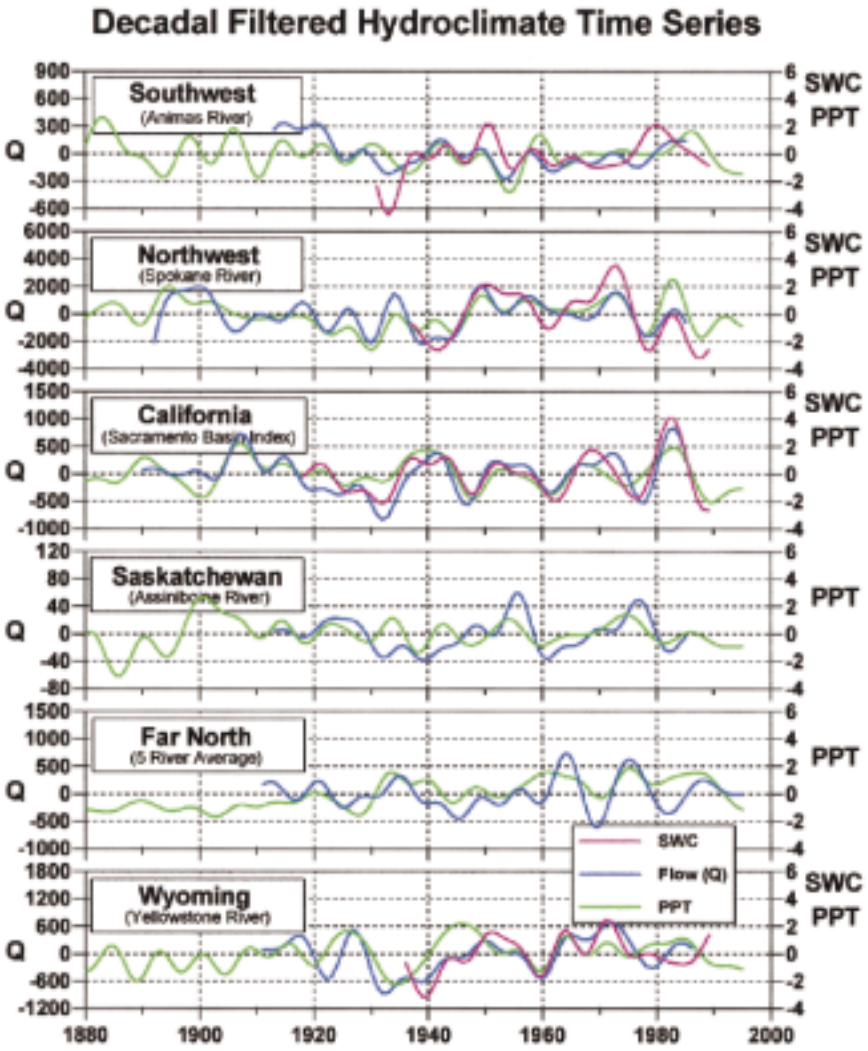

FIG. 4. RPCs of decadal precipitation (green) compared with snow accumulation (snow water equivalent, red) and stream discharge (blue) within the six RPC regions.

cedure reflect actual hydroclimatic fluctuations and are not artifacts of the particular precipitation data used.

c. Seasonality

For a given region, precipitation anomalies during certain seasons may contribute much more strongly than those during the rest of the year in producing decadal variability. To determine which months contribute most to decadal precipitation fluctuations, each decadal precipitation RPC series was correlated (Fig. 5) with unfiltered monthly precipitation anomaly series from a grid point at the center of its respective spatial loading pattern. For comparison with the climatological cycle, the long-term monthly mean precipitation at these centers is superimposed on each of graphs in Fig. 5.

In the Southwest, there are contributions to decadal variability during fall and winter in addition to summer, even though the seasonal cycle is peaked in late summer. In the Northwest, fall–winter contributions are greatest in producing decadal variability, strongly paralleling its seasonal cycle. Similarly, California has a strong winter contribution which is closely aligned with its strong mediterranean winter climatological pattern. Decadal precipitation variations in Saskatchewan are dominated by a broad warm season (spring–early fall) contribution, which is generally consistent with its summer seasonal maximum. The Far North is marked by contributions over several seasons (fall, winter, and summer), while its climatological mean pattern has a broad summer maximum. In Wyoming, largest contributions to decadal variability occur from June through November, while its climatology contains a decided May–June peak.

The makeup of these seasonal contributions was quite stable over the period of record, as indicated by a comparison of analogous correlations computed separately

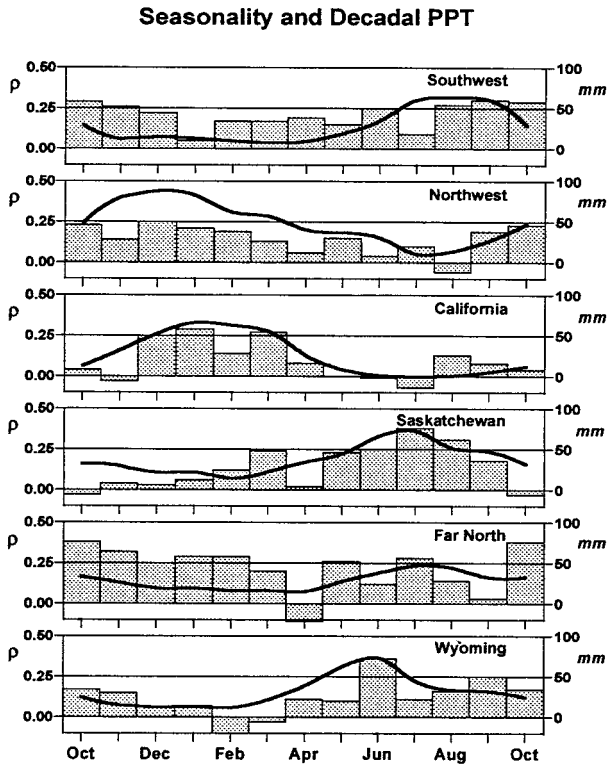

FIG. 5. Correlation (bars) of monthly unfiltered precipitation with decadal precipitation RPCs for selected monthly precipitation grid within each RPC region. For comparison, solid curve shows climatological monthly precipitation within each region.

from the first and second halves of the dataset. Generally, the seasonal contributions to decadal variability indicate that 1) decadal precipitation variation is often dominated by the months with largest climatological precipitation, but 2) the contributions are not restricted to the peak precipitation months, and 3) no single season (e.g., winter or spring) is the source of decadal variation over the whole western region. In the large perspective, both winter and summer contribute strongly to decadal variability.

4. Connection to atmospheric circulation

a. Association with decadal SLP field

To better understand their causes, we wish to know how patterns of decadal precipitation variability relate to atmospheric circulation. Therefore, we next employ the regional RPCs of the anomalous decadal precipitation in correlation analyses with global SLPs and (later) SSTs to address the following questions: Do decadal circulation linkages resemble their more familiar counterparts at monthly interannual timescales? Are the associated circulation patterns regional or global?

Fields of correlations between the decadal precipitation RPC amplitudes and decadal filtered SLP (Fig. 6) were mapped and examined to isolate possible causal mechanisms and links to regional and remote atmospheric circulations. These maps express the correlations between a particular RPC series and the decadal filtered SLP of each grid point. Later analyses employ the same tactic, but in relationship to decadal filtered SST. With the multiyear variability considered, there is considerable uncertainty in these correlations, which should probably be viewed without too much regard for their local levels of significance. However, to estimate the overall level of significance for a given correlation map (''field significance'') (Livezey and Chen 1983), a Monte Carlo exercise was conducted by gaging the area of significant correlation contained by the observed case against that of a set of 1000 synthetic correlation maps. To implement the Monte Carlo procedure, the sequence of observed annual mean SLP or SST anomaly maps was shuffled randomly and the resulting set of maps was then decadally filtered. The filtered synthetic sequences were then correlated with the unshuffled decadal precipitation RPCs to produce the 1000 different correlation maps. The original decadal precipitation RPCs were left intact to retain their meaning with respect to temporal and spatial variability; the original SLP and SST maps (spatial distribution of data) were also left intact to preserve spatial correlations, but the time sequences of these global maps were shuffled. Field significance was judged by counting the number of grid points in the observed map with higher positive (or lower negative) correlations than various threshold correlations, and gauging this number against corresponding counts from the sequence of synthetic maps. Confidence estimates from the Monte Carlo trials of correlations between the decadal precipitation RPCs and the SLP and SST fields are shown in Table 1. In the text, we report on the significance estimate based on the 0.5 correlation threshold; in general, these are consistent with those based on the other (0.3 and 0.7) correlation thresholds. The teleconnections of the decadal RPCs to atmospheric circulation vary widely in their spatial extent. Those of the Northwest (Fig. 6b) and California (not shown) RPCs are mostly confined to influences of regional-scale SLP anomalies. On the other hand, the Southwest and Saskatchewan RPCs are correlated (Figs. 6a,c) to decadal SLP anomalies on nearly global scales.

The Southwest decadal precipitation pattern is associated with a globally extensive SLP anomaly distribution (Fig. 6a). (For convenience, the correlations are discussed in terms of conditions associated with the wet phase of each western North American precipitation pattern; circulation associated with the dry phase would be opposite.) The field significance of this correlation map is high ($p < 0.05$). Wet conditions in the Southwest are most strongly related to anomalously low pressure south of the Aleutians. On a much broader scale, however, they are correlated to low pressure anomalies over the eastern Pacific/eastern America region in both the Northern and Southern Hemispheres; and to high pressure anomalies over much of the remainder of the

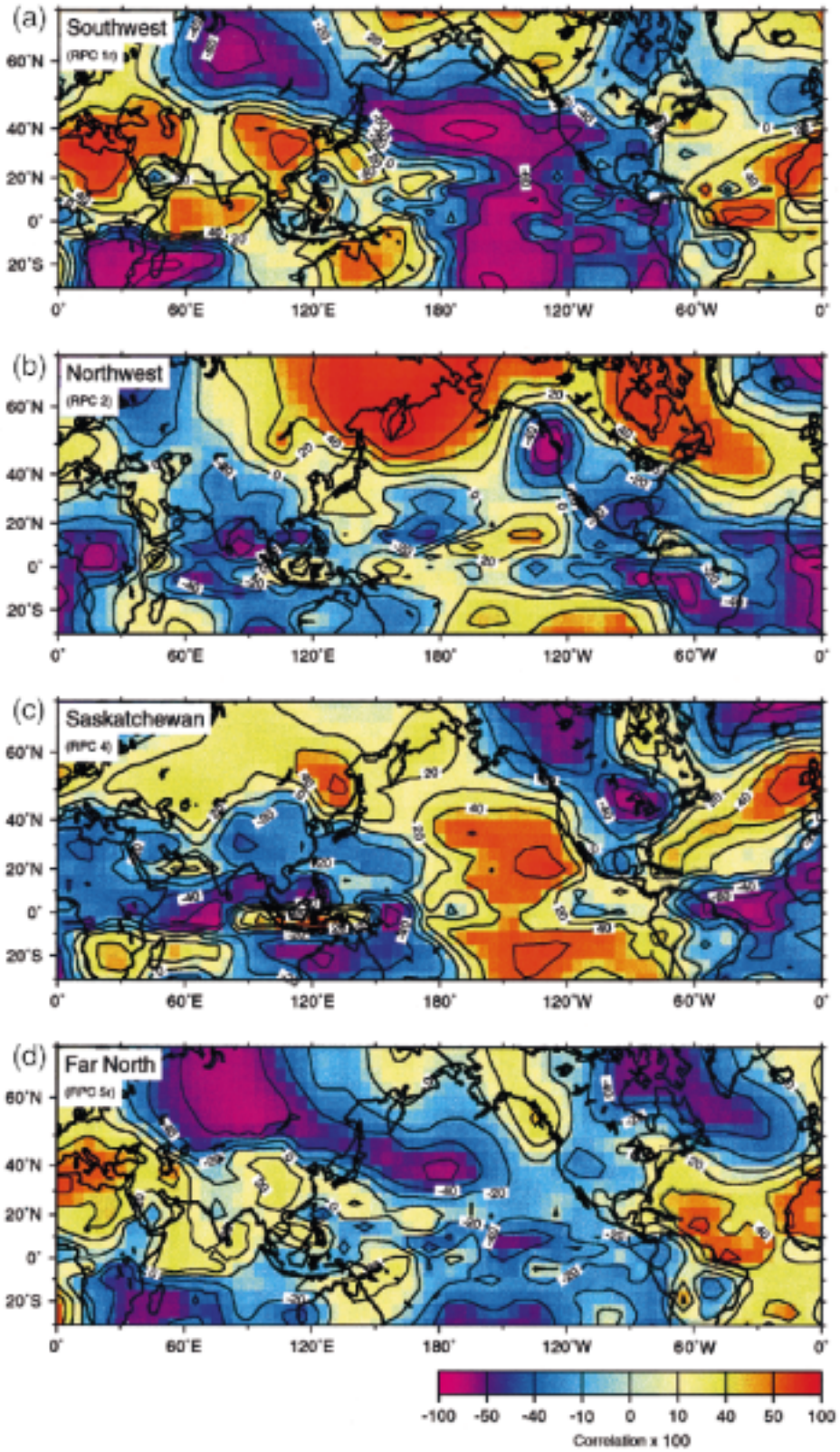

FIG. 6. (a)–(d) Correlation fields, decadal precipitation RPCs vs. SLP over global grid, 1951–93 for Southwest, Northwest, Saskatchewan, and Far North RPCs.

TABLE 1. Field significance levels (as p values)—correlation maps of decadal precipitation RPCs vs SLP, and SST for regions exceeding three correlation thresholds. Bold shading designates values exceeding the 95% significance level ($p < 0.05$).

Decadal precip RPC	SLP			SST		
	$\|\rho\| > 0.3$	$\|\rho\| > 0.5$	$\|\rho\| > 0.7$	$\|\rho\| > 0.3$	$\|\rho\| > 0.5$	$\|\rho\| > 0.7$
Southwest	0.056	**0.048**	**0.035**	**0.050**	**0.026**	**0.030**
Northwest	0.218	0.146	0.161	0.219	0.400	—
California	0.360	0.500	0.400	0.500	0.500	—
Saskatchewan	**0.043**	0.075	0.400	**0.023**	**0.037**	—
Far North	0.240	0.270	0.400	**0.001**	**0.001**	**0.001**
Wyoming	0.800	0.800	0.900	0.700	0.700	—

globe—particularly over Eurasia, the western Pacific, and the Indian Oceans. This global pattern resembles the classical Walker circulation—the Southern Oscillation in its warm, El Niño phase (Philander 1990). Thus, wet conditions in the Southwest have occurred during epochs with El Niño–like conditions, such as those in recent decades.

Decadal wet conditions in the Northwest are associated with a fairly strong regional low pressure center offshore in the easternmost Gulf of Alaska (Fig. 6b). Field significance for this map is not too high ($p < 0.15$), but the regional pattern provides an interesting contrast to the larger-scale ones for Southwest, Saskatchewan, and Far North. Among the apparent remote teleconnections, high pressure is situated to the north, centered over Kamchatka, northern Canada, and midlatitudes of the western North Atlantic. Interestingly, the low pressure anomaly correlated with decadal wet spells in the Northwest is similar to that which produces heavy seasonal precipitation (unfiltered) in the region (Klein and Bloom 1987) but in the decadal case, the anomalous low pressure is more confined to the eastern margin of the North Pacific.

Like the Southwest pattern, the wet phase of the Saskatchewan RPC has a strong global-scale link to the SLP field (Fig. 6c). Field significance is relatively high ($p < 0.08$). In closest proximity to the region, the pattern is associated with a swath of negative SLP anomalies extending to the northwest over Alaska and eastward into the Great Lakes. This regional anomaly structure presumably represents a long-term preference for cyclones to track from the Gulf of Alaska southeastward through western Canada. The most impressive aspect of the Saskatchewan circulation pattern, however, is its spatially extensive correlations, which literally span the globe. Later, it is shown that this pattern is consistent with broad-scale correlations to anomalous SST. Positive SLP anomalies over northern Asia and most of the eastern Pacific oppose the aforementioned regional anomalies over North America as well as a broad expanse of negative anomalies from South America, Africa, the Indian Ocean, Australia, and the western tropical Pacific. Except for North America, this pattern is quite opposite to the one for the Southwest RPC. Interestingly, the decadal precipitation anomalies in Saskatchewan can be mostly attributed to summer precipitation variability, in contrast to the more winter-dominated precipitation of the other regional RPC variations.

Far North SLP correlations (Fig. 6d) are not very impressive immediately over the Far North region itself, but carry a modest larger-scale signature. Field significance is not very impressive ($p < 0.27$) but because this decadal precipitation mode correlates strongly with SST, the SLP map is shown for comparison. Wet conditions in the Far North correlate with negative SLP anomalies in high northern latitudes, centered over Russia and eastern Canada. There are also correlations with low pressure at 20°–30°S over the South Pacific and over southern Africa and the eastern Indian Ocean. Correlations with high pressures occur in lower middle latitudes.

The Wyoming decadal precipitation RPC mode is weakly correlated to any large-scale circulation pattern, but wet conditions there are associated with high pressure anomalies over midlatitudes of the North Pacific and the North Atlantic. The Wyoming pattern is the only case without a well-developed low in the vicinity of the particular precipitation region.

b. Association with short-period circulation patterns

It seems appropriate to question: from what timescales are the decadal SLP correlations derived? Are the composite atmospheric circulation patterns in Fig. 6 produced by variations of a single atmospheric pattern, or are they the composite expression of several patterns? In examining such questions for a decadal shift in winter snow accumulation over the Rocky Mountains, Changnon et al. (1993) found that changes in four daily synoptic patterns were involved. In considering ENSO effects on winter precipitation over the western states, Cayan and Redmond (1994) identified five monthly North Pacific circulation patterns whose frequency of occurrence changed significantly between the warm and cool phases of the tropical Pacific.

Pursuing a similar strategy, an RPC analysis was conducted from unfiltered monthly gridded 700-mb height anomalies over the (20° to 70°N, 110°E to 65°W) sector of the Northern Hemisphere for all Novembers through March (NDJFM), 1947–92. These months were used because of the strong fall–winter–spring contribution to the decadal precipitation fluctuations at several of the precipitation regions (Fig. 5). Connections to monthly

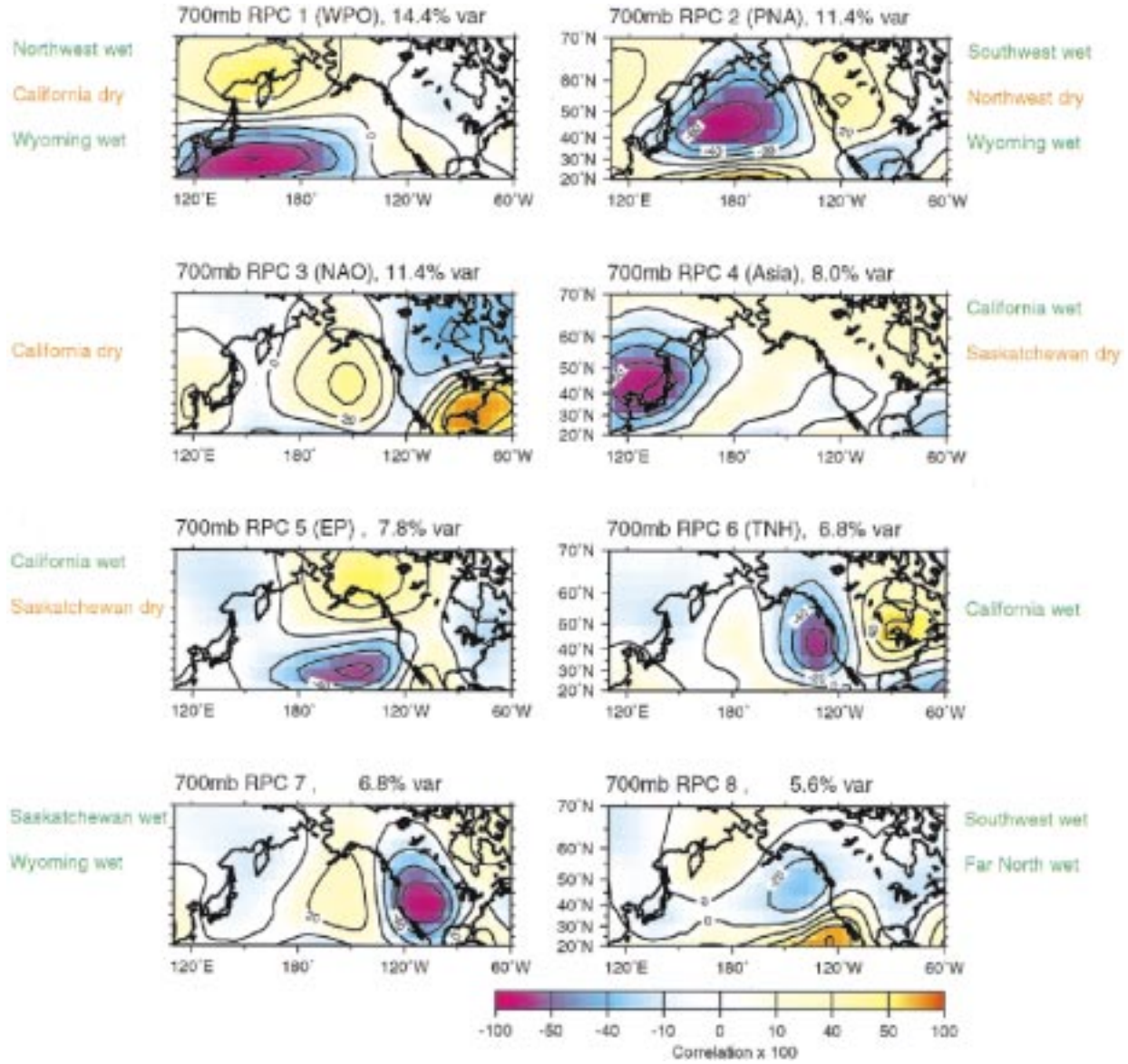

FIG. 7. Spatial loading patterns of monthly 700-mb height, NDJFM, 1947–92. Decadal precipitation tendencies associated with changes in frequency of each of these patterns is noted beside each.

scale variability, if present, should be particularly meaningful during NDJFM. Several of the resulting eight RPCs of monthly 700-mb height were recognized as having patterns identified by Wallace and Gutzler (1981) and BL in their classification of monthly Northern Hemisphere circulation types.

The eight primary monthly modes identified here are illustrated in Fig. 7, along with their contribution to the variance of 700-mb height anomalies over the entire space–time domain. RPC1 is identified as the West Pacific oscillation (WPO); RPC2 resembles the Pacific–North America (PNA) pattern; RPC3 appears to be a western accentuated version of the North Atlantic oscillation (NAO); RPC4 is an unnamed pattern centered over southeast China that we call the ''Asia'' pattern; RPC5 is the East Pacific (EP) pattern; RPC6 is the Tropical–Northern Hemisphere (TNH) pattern; RPC7 is an unnamed center over North America with a minor opposite phase structure to the west covering the eastern North Pacific; and RPC8 is an unnamed pattern that captures anomalous southeast-to-northwest gradients of pressure along the eastern North Pacific–western North America region. Differences between the present 700-mb height RPCs and those of BL can be explained by differences in datasets and methodology: BL's data are 1950–84 while ours are 1948–92; and BL analyzed time series of each month individually while ours are from a pooled 5-month block time series.

TABLE 2. Contingency tables between monthly circulation modes and decadal precipitation RPCs; χ^2 significance test provides for 2 × 2, 2 × 3 contingency tables. Bold shading indicates χ^2 significance at ≥90th percentile confidence level.

Decadal precip mode		700-mb monthly circulation modes																							
		WPO			PNA			NAO			ASIA			EP			TNH			RPC7			RPC8		
		+	−	n	+	−	n	+	−	n	+	−	n	+	−	n	+	−	n	+	−	n	+	−	n
Southwest	RPC1 +	7	9	30	**16**	**6**	**27**	9	10	27	8	8	30	12	8	26	17	11	18	9	13	24	**12**	**5**	**29**
	RPC1 −	11	11	28	**9**	**17**	**24**	11	8	31	8	11	31	10	15	25	13	11	26	7	13	30	**6**	**11**	**33**
	χ^2	0.1		1.0	**6.9**		**7.1**	0.4		0.5	0.2		0.3	1.8		2.2	0.2		1.8	0.2		0.8	**4.3**		**4.3**
Northwest	RPC2 +	**24**	**15**	47	**20**	**19**	**47**	20	21	45	19	15	52	21	13	52	19	16	51	25	18	43	23	20	43
	RPC2 −	**5**	**9**	21	**15**	**3**	**17**	11	6	18	7	5	23	8	6	21	9	11	15	8	11	16	9	5	21
	χ^2	**2.8**		2.9	**5.3**		**6.0**	1.2		1.2	0.0		0.3	0.1		0.1	0.4		3.2	1.4		1.6	0.5		1.4
California	RPC3 +	**5**	**16**	**24**	13	8	24	**7**	**11**	**27**	**13**	**7**	**25**	**12**	**6**	27	**15**	**7**	**23**	10	9	26	9	10	26
	RPC3 −	**17**	**13**	**45**	16	7	52	**24**	**10**	**41**	**10**	**21**	**44**	**12**	**18**	45	**13**	**18**	**44**	18	19	38	14	22	39
	χ^2	**5.4**		**6.1**	0.3		3.4	**4.9**		**5.1**	**5.3**		**5.5**	**3.2**		3.2	**3.6**		**4.3**	0.1		0.6	0.4		0.7
Saskatch.	RPC4 +	8	9	30	11	12	24	8	4	35	**7**	**8**	**32**	**5**	**18**	**24**	7	12	28	**9**	**8**	30	9	6	32
	RPC4 −	5	7	16	5	5	18	6	5	17	**0**	**11**	**17**	**6**	**5**	**17**	5	9	14	**3**	**10**	15	4	9	15
	χ^2	0.1		0.4	0.0		1.3	0.4		1.9	**6.9**		**7.8**	**3.7**		**4.1**	0.0		0.7	**2.7**		3.6	2.4		4.1
Far North	RPC5 +	25	32	82	36	20	83	26	30	83	29	24	86	33	30	76	32	34	73	31	36	72	**29**	**23**	**87**
	RPC5 −	1	6	11	6	3	9	3	6	9	7	4	7	3	2	13	5	3	10	3	5	10	**3**	**7**	**8**
	χ^2	2.3		2.2	0.0		0.6	0.5		1.3	0.3		3.9	0.1		2.1	0.6		0.6	0.2		0.3	2.2		**5.2**
Wyoming	RPC6 +	**18**	**13**	39	**18**	**8**	44	15	18	37	**13**	**13**	**44**	17	14	39	13	15	42	**19**	**13**	**38**	14	20	36
	RPC6 −	**4**	**9**	18	**4**	**7**	20	7	7	17	**1**	**13**	**17**	8	4	19	8	8	15	**3**	**11**	**17**	5	7	19
	χ^2	**2.7**		2.7	**3.5**		3.4	0.1		0.1	**7.3**		**8.4**	0.5		0.7	0.1		1.2	**5.6**		**5.6**	0.0		0.8

Changes in monthly atmospheric circulation patterns that are associated with the decadal precipitation RPCs were determined by compiling a census of the extremes of the monthly circulation patterns that occurred during extreme positive or negative phases of the six decadal precipitation RPCs. The census of extreme precipitation RPCs and extreme 700-mb height RPCs is summarized in four- and six-celled contingency tables. The 48 resulting contingency tables (the product of six decadal precipitation RPCs and eight monthly circulation modes) are shown in Table 2, along with estimates of the statistical likelihood that the counts are different from chance occurrence. The significance of the observed counts was judged using the χ^2 statistic (Spiegel 1961) for both the distribution of the extreme categories (2 × 2 tables) and the distribution of the extreme plus the neutral categories (2 × 3 tables), where neutral cases refer to coincidences of extremes of precipitation RPCs with nonextreme 700-mb height RPCs. Extremes of the regional precipitation patterns were designated as periods when the magnitude of their RPC amplitudes exceeded 1.0; intervals satisfying this criteria amount to about one-third of the time within the 1948–92 period. Extremes of the monthly circulation pattern were identified by a similar criterion (monthly 700-mb height RPC amplitude exceeds 0.8); months satisfying this criterion total about 30%–50% of the 1948–92 time interval. The χ^2 statistic is sensitive to linear associations that would show up in opposing fashion during the two extremes of decadal precipitation (e.g., the wet associates with a higher frequency of ''+'' phase events and the dry associates with a higher frequency of ''−'' phase events in the monthly circulation mode). Note, however, that nonlinear associations also can be detected by this test. For example, one of the four cells may contain an unusual number (high or low) of counts, while the other three cells have an ''average'' number. The veracity of these results is suggested by two different indications: 1) the χ^2 values from the 2 × 2 tables of the extreme categories were generally consistent with the results of an analogous chi-square test of a 2 × 3 contingency table; 2) the estimated levels of statistical significance on the contingency tables were consistent with a set of χ^2 values determined for 1000 Monte Carlo trials in which the time series of monthly circulation mode amplitudes were shuffled randomly to produce a separate contingency table for each trial.

With the exception of the Far North precipitation pattern, each decadal precipitation RPC appears to associate (beyond chance occurrences) with at least two monthly circulation modes (Table 2). Significant relations to the various decadal precipitation modes are summarized alongside the circulation mode maps in Fig. 7. The Southwest precipitation pattern associates significantly with the deep Aleutian low phase of the PNA mode and with the strong subtropical high–deep North Pacific low phase of RPC8. Not surprisingly, each of these patterns favors a southward displacement of Pacific storm activity southward into the Southwest. The Northwest precipitation pattern also associates significantly with two circulation modes which presumably are key in accentuating or weakening the tendency for a Pacific Northwest–oriented storm track. The Northwest wet phase corresponds with the low subtropical pressure–low Kamchatka pressure phase of the WPO pattern, and with the weakened Aleutian low phase of

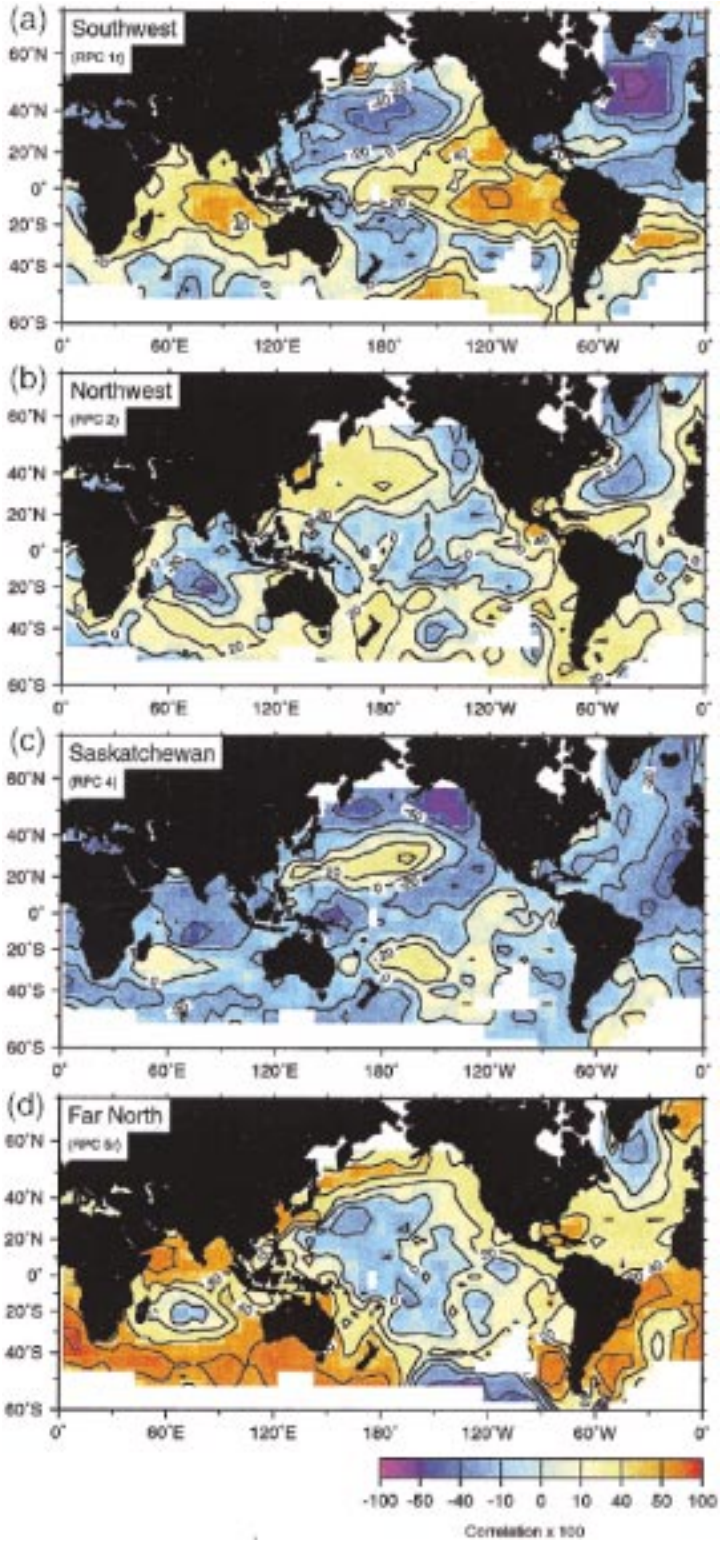

FIG. 8. (a)–(d) Correlation fields, decadal precipitation RPCs vs SST over global grid, 1900–91 for Southwest, Northwest, Saskatchewan, and Far North RPCs.

the PNA pattern. The frequency of occurrence of strong PNAs, however, is not much different between wet and dry epochs of Northwest precipitation. Presumably, these modes are key in accentuating or weakening the long-term tendencies for a Pacific Northwest-oriented storm track. Decadally wet phases of the California precipitation pattern are associated with four NJDFM circulation modes: the high subtropical pressure–low Kamchatka pressure phase of the WPO pattern (like the Southwest), the low Southeast pressure form of the NAO pattern, to the low pressure form of the Asia pattern, and to the low pressure eastern North Pacific form of the EP pattern. Each of these patterns favors more frequent North Pacific winter storms moving into California. The Saskatchewan precipitation pattern is associated significantly with three different circulation modes. The Saskatchewan dry phase corresponds to more frequent occurrences of the low pressure form of the Asia pattern (note that only the dry phase shows a distinction; the wet phase does not associate with a significant change in frequency between either phase of the Asia pattern). The Saskatchewan wet phase corresponds to more frequent occurrences of the high North Pacific pressure form of the EP pattern (the dry phase shows little association). The Saskatchewan dry phase also associates quite strongly with the positive North American pressure form of RPC7 (but the wet phase shows little distinction between either form of RPC7). The Wyoming decadal precipitation pattern associates significantly to four different monthly circulation modes. Its wet phases corresponds to the low subtropical pressure–high Kamchatka pressure phase of the WPO pattern, to the deep Aleutian low phase of the PNA pattern, and to the deep North America low pressure form of RPC7. The dry phase of the Wyoming pattern corresponds to more frequent occurrences of the high-pressure form of the Asia pattern, but its wet phase does not show a distinct connection to this mode. Curiously, the Far North decadal precipitation pattern does not relate strongly to any of the monthly circulation modes, though there is a hint that wet conditions may associate with the high subtropical pressure form of RPC8.

Thus, the SLP correlation patterns in Fig. 6 correspond, in part, to fluctuations in atmospheric circulation on more familiar monthly timescales. In particular, there is evidence that the regional decadal precipitation anomalies result at least partially from slow changes in the frequencies of several shorter period modes of circulation. Four of the monthly circulation patterns (PNA, WPO, TNH, and EP) have been associated with ENSO conditions (Livezey and Mo 1987; Cayan and Redmond 1994). That these same modes are involved in regional decadal precipitation fluctuations suggests that similar processes may operate on both ENSO and decadal timescales. This similarity lends evidence to the proposition that tropical conditions affect midlatitude decadal precipitation variability.

5. Connections to SST

We can expect decadal precipitation to be linked to SST anomaly variations because the SST field has distinct decadal fluctuations (Miller et al. 1994; Mantua et al. 1997; White et al. 1997; Livezey and Smith 1998) and is so strongly tied to climate variability. Also, SST may share connections to atmospheric circulations that produce precipitation fluctuations. In conjunction with the SLP patterns from the previous section, these SST associations should help to elucidate driving mechanisms, and to determine if the precipitation ''signals'' are regionally derived or involve large-scale climate anomalies. Possible links between SST anomaly patterns and decadal precipitation are examined by using correlations. The correlation fields (Figs. 8a–d) are analogous to those with SLP, except that longer series are employed (1900–91) in computing the correlations.

The SST connection to the Southwest decadal precipitation RPC (Fig. 8a) is nearly global and in agreement with the global-scale SLP anomalies in Fig. 6a. This correlation map has a high degree of field significance ($p < 0.03$). For the wet phase of Southwest decadal precipitation, the SST pattern has warm anomalies extending over the eastern Pacific, Indian, and South Atlantic; and cool anomalies over the western and central North Pacific, North Atlantic, and Mediterranean Sea. In the Pacific, the tongue of anomalous warm water in the eastern tropical Pacific extends poleward along the North America and South America coasts and is similar to that which occurs during the El Niño phase of ENSO, as are the cool SST anomalies in the midlatitudes of the North and South Pacific. The presence of somewhat symmetrical Northern-to-Southern Hemisphere decadal modes of SST and atmospheric variability has also been demonstrated in a global analysis of observed SST, upper-ocean heat content, pressure, and wind datasets (Xu 1993).

For the Northwest decadal precipitation RPC, strongest SST connections (Fig. 8b) are remote, but overall field significance is low ($p < 0.40$). During the wet phase of Northwest decadal precipitation, there are warm anomalies over the western North Pacific and Gulf of Mexico, as well as across the 30°–40°N zone spanning the Pacific; in portions of the Indian and Atlantic basins, La Niña–like cool SSTs along the Tropics in the central Pacific and Indian Oceans are weakly associated with long-term wet Northwest conditions. This general pattern of SST is consistent with the finding of Mantua et al. (1997) that in the interior Northwest, interannual variability of anomalous snow accumulation (Cayan 1996) is closely related to the major pattern of interdecadal oscillation in the North Pacific, whose deep Aleutian low phase has cool SST anomalies in the west and central North Pacific of opposite sign to those along the eastern boundary.

The SST pattern associated with the Saskatchewan decadal precipitation RPC (Fig. 8c) are of uniform sign

over much of the world ocean, consistent with its globally distributed SLP anomaly pattern (Fig. 6c). Field significance is high ($p < 0.04$). Wet decades in Saskatchewan are associated with cool conditions globally except for out-of-phase warm pools in the western subtropical regions of the North Pacific, South Pacific, and North Atlantic. The Saskatchewan SST correlation pattern is somewhat similar to the pattern associated with the Southwest precipitation, but has the opposite sign (i.e., more like the La Niña phase of the Southern Oscillation). These opposite signs are consistent with the inverse relation between their respective SLP correlation patterns.

Perhaps the most perplexing link between decadal precipitation and SST is that of the Far North precipitation RPC (Fig. 8d). The structure of the SST correlation pattern is quite strong and global, with warmer SSTs across much of Northern Hemisphere and especially the Southern Hemisphere associated with higher Far North precipitation. Field significance is very high ($p < 0.001$). The temporal variation of the Far North RPC time series is trendlike, containing most of its increase between 1910 and 1940. This trend is similar to the increase seen in global temperature (IPCC 1996, 142). The SLP correlations (Fig. 6d) do not register as strongly significant, but they are calculated over a more limited (1951–92) period which does not include the major change between 1910 and 1940.

SST correlations are reasonable reflections of the corresponding scales and patterns displayed by the SLP correlation analyses. To confirm and perhaps to sharpen the SST correlations, a canonical correlation (CCA) analysis (Graham 1994) was performed to extract joint pairs of predictors (decadal SST fields) and predictands (decadal precipitation fields) on decadal timescales. This analysis captures the greatest amount of covariability by a linear combination of a given number of predictor and predictand data. Twelve global SST EOFs and six western North America precipitation EOFs, each from decadally filtered data, were employed as the predictor–predictand datasets. Each mode has a spatial pattern and associated time varying amplitudes for both predictor and predictand. The correlation between the respective predictor and predictand time amplitudes is referred to here as the canonical correlation. In this case, we show the pair of patterns having the strongest canonical correlation; other modes were broadly related to the decadal precipitation RPCs and their respective SST correlation patterns. The leading decadal CCA mode (Fig. 9a) has a canonical correlation of 0.85, and its spatial predictor–predictand maps are very similar to the Southwest RPC spatial loading pattern (Fig. 3, top) and its associated SST correlation map (Fig. 8a). The reemergence of these patterns seems to confirm the robust nature of the Southwest pattern and its global SST connections, emphasizing the certainty of a global SST connection, including strong tropical weighting.

For comparison to the decadal SST-precipitation CCA modes, the same CCA exercise was conducted, but for ENSO-filtered (3–7-yr period) filtered data. Again, the most impressive canonical correlation pattern that emerged from this analysis (Fig. 9b) is also a Southwest precipitation pattern, which is associated with a global SST anomaly structure, especially in the Indian and Pacific Oceans. The canonical correlation for this mode pair is 0.56. The key point here is that the pattern has a similar tropical distribution and global SST connection (warm tropical SST produces heavy southwest precipitation) as does the decadal canonical correlation. This suggests that similar large-scale physical mechanisms operate on both decadal and ENSO timescales.

6. Global precipitation linkages

Considering the large-scale connections of several of the decadal precipitation patterns with circulation and SST, we suspect that these precipitation regional patterns actually may be parts of organized precipitation anomalies on a much larger scale. A number of studies have pointed to very large-scale interdecadal modes as an influence on global climate (e.g., Latif and Barnett 1994; Miller et al. 1994; Mantua et al. 1997; Livezey and Smith 1998). For example, low-frequency fluctuations of snow accumulation over the Idaho and Montana region were noted by Mantua et al. (1997) to reflect a large-scale interdecadal SST and atmospheric circulation over the Pacific basin. This connection shows up rather weakly in the present results, but it may be obscured by our use of all months of the year in the analyses undertaken here, rather than just the winter season's precipitation. An analysis of decadal precipitation over all available global land area was performed next in order to place these North American modes into larger-scale context.

The regional decadal precipitation patterns with the most impressive global SST and SLP connections is the Southwest pattern. A rotated EOF of land precipitation yields a global precipitation mode that incorporates the decadal character of precipitation in the Sahel (Fig. 10a), as well as the essence of the Southwest mode found in the regional analysis. The global precipitation mode and its association with circulation and SST indicates the tendency for the Southwest precipitation to be out-of-phase with that over the Sahel. Comparison of the respective precipitation RPCs (Fig. 10b) also suggests a close correspondence between the Southwest decadal precipitation mode and the global Sahel precipitation pattern, and the tendency for Southwest to be wet while the Sahel and other remote regions are dry. An EOF analysis of monthly unfiltered precipitation over global land by Diaz (1996) finds a similar spatial configuration of global precipitation and its corresponding time series. Re-

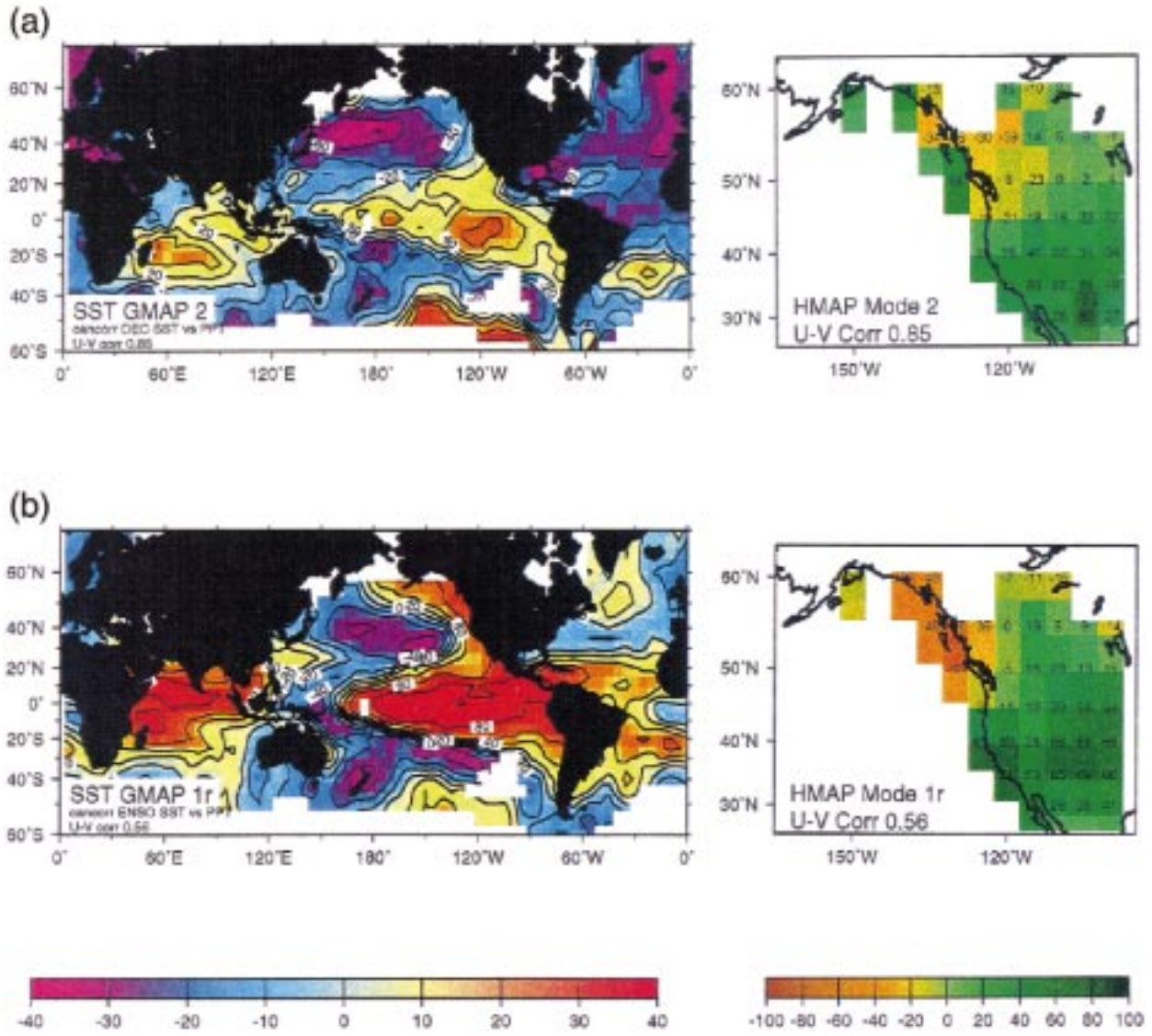

FIG. 9. (a) Canonical correlation pair, decadal SST (GMAP) and decadal precipitation (HMAP) for strongest canonical correlation mode. Spatial patterns are expressed as correlations between the time varying amplitudes and the original decadal time series at each grid point. (b) Same as (a), but for ENSO-filtered data.

lated circulation and SST patterns produced by correlating SLP and SST maps (as before) with the global precipitation RPC in Fig. 10b are very similar to the correlation maps shown for the Southwest decadal RPC in Figs. 6a and 8a. The circulation pattern (SLP correlation) clearly involves the global Tropics as well as the midlatitudes, with in-phase SLP anomalies over the eastern Pacific and the Americas, and out-of-phase anomalies over Eurasia and the western Pacific. It is noteworthy that this pattern of SLP anomalies, as well as the associated one for SST, is associated with north–south displacements of decadally varying zonally averaged precipitation along the West Coast (Dettinger et al. 1998). The SST anomaly pattern favoring wet decades over the Southwest (Fig. 8a) has warm SST anomalies over the tropical Pacific and Indian Oceans, and cool SST in the western North Pacific and North Atlantic. This SST pattern strongly resembles the global SST anomaly pattern identified by Folland et al. (1991) as a major component of the global climate condition associated with swings in the Sahel precipitation. It seems that a chain of associated precipitation fluctuations separated by half the earth's circumference is connected by slow changes in large scale climate anomaly patterns involving circulation features resembling the Walker circulation (Khandekar 1991) as well as global SST anomalies. An intriguing feature is that in the Southwest these large-

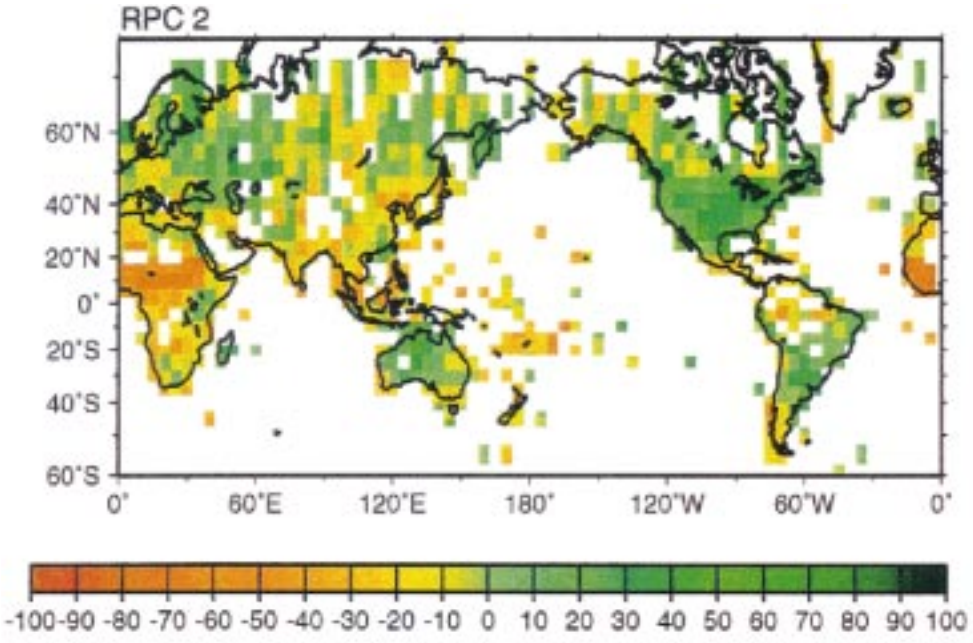

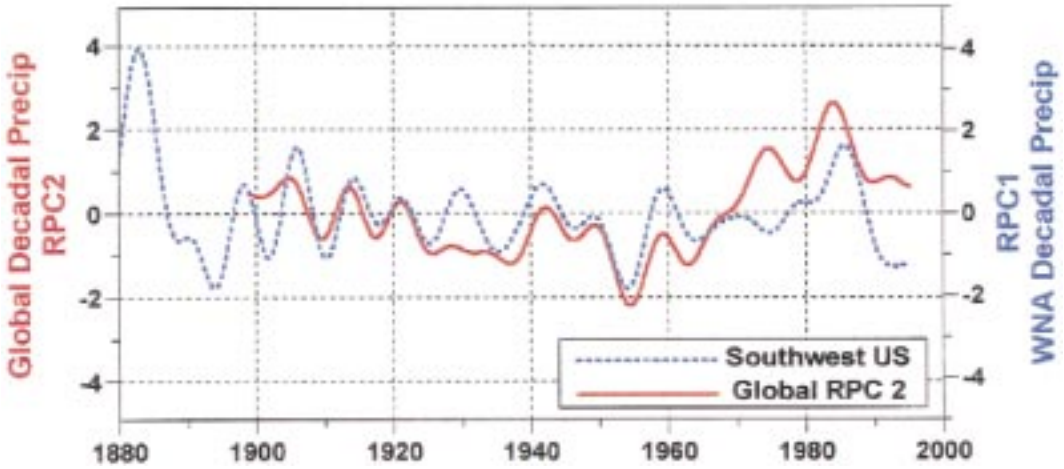

FIG. 10. Second RPC of global decadal filtered land precipitation has spatial loadings (top) with southwest United States out-of-phase with that over North African Sahel region. The time series of this RPC compares well with that of RPC 1 (southwest pattern) of western North America decadal precipitation.

scale patterns modulate winter and summer precipitation systems, despite their very different character (see Webb and Betancourt 1990).

7. Conclusions

The present study adds to a body of evidence that regional precipitation undergoes important variations over decadal epochs. In the western North America region examined here, decadal fluctuations (periods of 7 yr and longer) account for 20%–45% of the annual precipitation variance. Decadal precipitation fluctuations are matched fairly closely to those of independent observations of snowpack and streamflow, so it seems that the historical precipitation station network is capable of recording the essence of these low-frequency variations with some fidelity.

The low-frequency precipitation variability is a com-

plex mixture, however, as different seasons dominate decadal precipitation anomalies in the different areas of the West. Moreover, it is clear that, within a season, several types of weather patterns contribute to anomalous precipitation accumulations over these many-year periods. Finally, complexity is added because the spatial scale of decadal precipitation anomalies is generally not continental, but rather regional, spanning distances on the order of 1000 km. In examining zonal averages of decadal and ENSO precipitation anomalies along the west coast of North America, Dettinger et al. (1998) show that these fluctuations can be described as mostly latitudinal redistributions with smaller changes in the overall amount of precipitation. The regional nature of precipitation variability discussed here was based on a rotated principal components analysis (RPC) as a convenient means of extracting covarying patterns. These results are consistent with other studies of low-frequency hydrological variability over parts of North America—for example the patterns uncovered here correspond well with those described in Meko et al. (1993) study of moisture and tree ring variability over the conterminous United States, and those found by Guetter and Georgakakos (1993) and Lins (1997) in runoff and streamflow patterns over the conterminous United States. That it tends to be confined to more regional packets than other, more frequently studied climate measures like temperature is an important distinction of the hydrological variability: precipitation is a regionally varying field subject to higher-order atmospheric spatial structure on timescales ranging from days to the decadal periods considered here. The regional scales of decadal precipitation variations identified in western North America do not, however, preclude some larger-scale signals. Indeed, the Southwest pattern appears to be a part of a much larger precipitation (and climate) pattern that encompasses much of the earth, with important ties to the Sahel and other distant regions.

What causes the interdecadal variability of precipitation over this region? The atmospheric circulation plays a lead role, and correlations of the precipitation ''modes'' with decadal filtered sea level pressure (SLP) anomalies reveal regional-to larger- scale anomaly signatures similar to those producing short period (monthly-to-interannual) precipitation fluctuations (e.g., Namias 1978, 1979; Klein and Bloom 1987; Cayan and Peterson 1989). In particular, precipitation patterns over the southwestern United States and the Canadian prairies appear to involve global shifts in atmospheric pressure, with strong correlations extending into the Tropics and Southern Hemisphere. Anomalies of global SST are also involved with these decadal precipitation fluctuations, and results are consistent with the linkages to the atmospheric circulation. In the atmosphere, we can begin to detect the nature of some of these decadal associations by cataloging the frequencies of occurrence of common winter circulation patterns during extremes of each particular decadal precipitation RPC. Rather than being forced by a single low-frequency circulation mode, the decadal precipitation anomalies often result from changes in occurrence of several higher-frequency circulation patterns. More than one monthly circulation pattern contributes to the decadal variability of each decadal precipitation mode. Evidently the overall long period circulation signature in decadal precipitation is a mix of these shorter period circulation patterns. Four of these monthly circulation patterns—PNA, WPO, EP, and TNH—also are modulated by ENSO conditions. By inference, this further suggests a tropical–global influence upon low-frequency precipitation variability in western North America. Decadal precipitation fluctuations over the Pacific Northwest, California, and Wyoming correlate with nearby regional scale circulation anomaly patterns. One interpretation of these more regionally confined patterns is that the patterns involved are truly regional in scale. A more likely explanation is that the overall decadal correlations represent an amalgam of several short period anomaly patterns having differing large-scale teleconnections, which intersect so that the given region receives its precipitation from a different mix of large-scale circulation patterns.

Does the anomalous SST drive the low-frequency precipitation fluctuations? The correlation fields shown above are not conclusive, but they suggest that there is a cause–effect linkage between SST anomalies and some of the low-frequency precipitation patterns noted above. One interpretation, which might be tested with general circulation model experiments is that persistent, large-scale SST anomalies nudge the atmospheric circulation toward certain forms of preferred modes, such as the monthly pattern discussed above. Supporting evidence for this linkage is 1) massive (global scale) SST anomaly shifts are involved, and 2) for at least one of the decadal precipitation modes discussed here, the Southwest RPC, there is a similarity in the spatial scale of the associated SST anomalies on decadal scales with those on ENSO scales. This feature is consistent with other evidence that finds similarities between ENSO and decadal patterns (Zhang et al. 1997; White et al. 1996). Thus, it seems likely that a coupled ocean–atmosphere system is involved in producing prominent patterns of low-frequency precipitation variability. The hypothesis that persistent SST anomaly patterns condition the extratropical atmosphere toward certain circulation modes has been validated with general circulation models, and the present results would benefit from further testing.

Available records indicate that a substantial portion of the natural variability of precipitation is in the decadal range. Most of the instrumental records available for the study of interdecadal climate variability are less than 100 yr in length. Most of the correlations obtained with the SLP and SST fields are based on too few degrees of freedom to be strictly significant. However, the patterns are evocative and are sufficiently familiar from shorter time scale connections to be convincing. Some of the uncertainties (tentativeness) of results in this anal-

ysis derives from the fact that these low-frequency fluctuations, which Karl (1988) called the ''gray area of climate variability,'' are not described very well by our relatively short instrumental records. These shortcomings could be mitigated by the development and interpretation of proxy climate records and the evolution of realistic model simulations that contain the essential elements of these low-frequency timescales.

Acknowledgments. We thank Jon Eischeid for data preparation, Emelia Bainto, Larry Riddle, and Marguerette Schultz for illustrations, and Nicki Pyles for word processing. Bob Livezey and two anonymous reviewers provided comments that were very useful in focusing and sharpening the manuscript. The PACLIM Workshop provided a forum for the initial presentation of this material. We thank the USGS Global Change Hydrology program for support of MDD; Paleoclimatology section of NOAA's Office of Global Programs, Grant NOAA NA56GPO404 for support of HFD, MDD, and DRC; the NOAA Experimental Climate Prediction Center at Scripps Institution of Oceanography and the Scripps/Lamont Consortium for support of DRC and NEG; and the NSF Climate Dynamics Program, Grant ATM-9509780 for support of DRC.

REFERENCES

Aguado, E., D. R. Cayan, L. Riddle, and M. Roos, 1992: Climatic fluctuations and timing of West Coast streamflow. *J. Climate,* **5,** 1468–1483.

Barnett, T. P., K. Brennecke, J. Limm, and A. M. Tubbs, 1984: Construction of a near-global sea-level pressure field. Scripps Institution of Oceanography Reference Series 84-7, 35 pp. [Available from Scripps Institution of Oceanography, La Jolla, CA 92093-0224.]

Barnston, A. G., and R. E. Livezey, 1987: Classification, seasonality, and persistence of low-frequency atmospheric circulation patterns. *Mon. Wea. Rev.,* **115,** 1083–1126.

Cayan, D. R., 1996: Interannual climate variability and snowpack in the western United States. *J. Climate,* **9,** 928–948.

——, and D. H. Peterson, 1989: The influence of North Pacific atmospheric circulation on streamflow in the West. *Aspects of Climate Variability in the Pacific and the Western Americas, Geophys. Monogr.,* No. 55, Amer. Geophys. Union, 375–397.

——, and K. T. Redmond, 1994: ENSO Influences on atmospheric circulation and precipitation in the western United States. *Proc. 10th Annual Pacific Climate (PACLIM) Workshop,* Pacific Grove, CA, 5–26. [Available from California Department of Water Resources, Interagency Ecological Studies Program, P.O. Box 942836, Sacramento, CA 94236-0001.]

Changnon, D., T. B. McKee, and N. J. Doesken, 1993: Annual snowpack patterns across the Rockies: Long-term trends and associated 500-mb synoptic patterns. *Mon. Wea. Rev.,* **121,** 633–647.

Dettinger, M. D., and D. R. Cayan, 1995: Large-scale atmospheric forcing of recent trends toward early snowmelt runoff in California. *J. Climate,* **8,** 606–623.

——, and D. S. Schaefer, 1995: Decade-scale hydroclimatic forcing of ground-water levels in the central Great Basin, eastern Nevada. *Proc. American Water Resources Association Annual International Symp.,* Herndon, VA, 195–204.

——, D. R. Cayan, H. F. Diaz, and D. M. Meko, 1998: North–south precipitation patterns in western North America on interannual-to-decadal time scales. *J. Climate,* **11,** 3095–3111.

Diaz, H. F., 1996: Precipitation monitoring for climate change detection. *Meteor. Atmos. Phys.,* **60,** 179–190.

——, and G. N. Kiladis, 1992: Atmospheric teleconnections associated with the extreme phase of the Southern Oscillation. *El Nino: Historical and Paleoclimatic Aspects of the Southern Oscillation,* H. F. Diaz and V. Markgraf, Eds., Cambridge University Press, 7–28.

Douglas, A. V., D. R. Cayan, and J. Namias, 1982: Large-scale changes in North Pacific and North American weather patterns in recent decades. *Mon. Wea. Rev.,* **110,** 1851–1862.

Eischeid, J. K., H. F. Diaz, R. S. Bradley, and P. D. Jones, 1991: A comprehensive precipitation data set for global land areas. Carbon-Dioxide Research Program Rep. DOE/ER-69017T-II1, TR051, United States Department of Energy, 81 pp.

——, C. B. Baker, T. R. Karl, and H. F. Diaz, 1995: The quality control of long-term climatological data using objetive data analysis. *J. Appl. Meteor.,* **34,** 2787–2795.

Ely, L. L., Y. Enzel, and D. R. Cayan, 1994: Anomalous North Pacific atmospheric circulation and large winter floods in the southwestern United States. *J. Climate,* **7,** 977–987.

Folland, C. K., J. A. Owen, M. N. Ward, and A. W. Colman, 1991: Prediction of seasonal rainfall in the Sahel region using empirical and dynamical methods. *J. Forecasting,* **10,** 21–56.

Graham, N. E., 1994: Decadal-scale climate variability in the tropical and North Pacific during the 1970s and 1980s: Observations and model results. *Climate Dyn.,* **10,** 135–162.

Groisman, P. Ya., and D. R. Legates, 1994: The accuracy of United States precipitation data. *Bull. Amer. Meteor. Soc.,* **75,** 215–227.

Guetter, A. K., and K. P. Georgakakos, 1993: River outflow of the conterminous United Sates, 1939–1988. *Bull. Amer. Meteor. Soc.,* **74,** 1873–1891.

Horel, J. D., 1981: A rotated principal component analysis of the interannual variability of the Northern Hemisphere 500-mb height field. *Mon. Wea. Rev.,* **109,** 2080–2092.

Hughes, M. K., and P. M. Brown, 1992: Drought frequency in central California since 101 B.C. recorded in giant sequoia tree rings. *Climate Dyn.,* **6,** 161–167.

IPCC, 1996: *Climate Change 1995: The Science of Climate Change.* Cambridge University Press, 584 pp.

Karl, T. R., 1988: Multi-year fluctuations of temperature and precipitation; the gray areas of climate change. *Climate Change,* **12,** 179–197.

Kaylor, R. E., 1977: Filtering and decimation of digital time series. University of Maryland Tech. Rep. Note BN 850, 14 pp. [Available from Engineering and Physical Science Library, University of Maryland at College Park, College Park, MD 20740.]

Khandekar, M. L., 1991: Eurasian snow cover, Indian monsoon and El Niño/Southern Oscillation—A synthesis. *Atmos.–Ocean,* **29,** 636–647.

Klein, W. H., and H. J. Bloom, 1987: Specification of monthly precipitation over the United States from the surrounding 700-mb height field. *Mon. Wea. Rev.,* **115,** 2118–3132.

Langbein, W. B., and J. R. Slack, 1982: Yearly variations in runoff and frequency of dry years for the conterminous United States, 1911–79. U.S. Geological Survey Open-File Rep. 82-751, 85 pp. [Available from U.S. Geological Survey, Reston, VA 22092.]

Latif, M., and T. P. Barnett, 1994: Causes of decadal climate variability over the North Pacific and North America. *Science,* **266,** 634–637.

Lins, H. F., 1997: Regional streamflow regimes and hydroclimatology of the United States. *Water Resour. Res.,* **33,** 1655–1667.

Livezey, R. E., and W. Y. Chen, 1983: Statistical field significance and its determination by Monte Carlo techniques. *Mon. Wea. Rev.,* **111,** 46–59.

——, and K. C. Mo, 1987: Tropical–extratropical teleconnections during the Northern Hemisphere winter. Part II: Relationships between monthly mean northern hemisphere circulation patterns and proxies for tropical convection. *Mon. Wea. Rev.,* **115,** 3115–3132.

——, and T. M. Smith, 1998: Covariability of aspects of North Amer-

ican climate with global sea surface temperatures on interannual to interdecadal time scales. *J. Climate,* in press.

Mantua, N. J., S. R. Hare, Y. Zhang, J. M. Wallace, and R. C. Francis, 1997: A Pacific interdecadal climate oscillation with impacts on salmon production. *Bull. Amer. Meteor. Soc.,* **78,** 1069–1079.

Meko, D., E. R. Cook, D. W. Stahle, C. W. Stockton, and M. K. Hughes, 1993: Spatial patterns of tree-growth anomalies in the United States and southeastern Canada. *J. Climate,* **6,** 1773–1786.

Miller, A. J., T. P. Barnett, D. R. Cayan, N. E. Graham, and J. M. Oberhuber, 1994: The 1976–77 climate shift of the Pacific Ocean. *Oceanography,* **7,** 21–26.

Namias, J., 1978: Multiple causes of the North American abnormal winter 1976–77. *Mon. Wea. Rev.,* **106,** 279–295.

——, 1979: Premonitory signs of the 1978 break in the West Coast drought. *Mon. Wea Rev.,* **107,** 1675–1681.

Parker, D. E., M. Jackson, and E. B. Horton, 1995: The GISST2.2 sea surface temperature and sea-ice climatology. Climate Research Tech. Note CRTN 63, 16 pp. [Available from Hadley Centre, Meteorological Office, London Road, Bracknell, Berkshire RG12 2SY, United Kingdom.]

Philander, S. G., 1990: *El Niño, La Niña, and the Southern Oscillation.* Academic Press, 289 pp.

Pyke, C. B., 1972: Some meteorological aspects of the seasonal distribution of precipitation in the Western United States and Baja, California. UCAL-WCR-W-254, University of California, Water Resources Center, 205 pp.

Redmond, K. T., and R. W. Koch, 1991: Surface climate and streamflow variability in the western United States and their relationship to large scale circulation indices. *Water Resour. Res.,* **27,** 2381–2399.

Richman, M. B., 1986: Rotation of principal components. *J. Climatol.,* **6,** 293–335.

Roos, M., 1991: A trend of decreasing snowmelt runoff in northern California. *Proc. 59th Western Snow Conference,* Juneau, AK, 29–36.

——, 1994: Is the California drought over? *Proc. 10th Annual Pacific Climate (PACLIM) Workshop,* Pacific Grove, CA, 123–128. [Available from California Department of Water Resources, Interagency Ecological Studies Program, P.O. Box 942836, Sacramento, CA 94236-0001.]

Ropelewski, C. F., and M. S. Halpert, 1986: North American precipitation and temperature patterns associated with the El Niño/Southern Oscillation (ENSO). *Mon. Wea. Rev.,* **114,** 2352–2362.

Sellers, W. D., 1968: Climatology of monthly precipitation patterns in the western United States, 1931–1966. *Mon. Wea. Rev.,* **96,** 585–595.

Spiegel, M. R., 1961: *Statistics*. Schaum's Outline Series in Mathematics, McGraw-Hill, 359 pp.

Stahle, D. W., and M. K. Cleveland, 1988: Texas drought history reconstructed and analyzed from 1698 to 1980. *J. Climate,* **1,** 59–74.

Stine, S., 1994: Extreme and persistent drought in California and Patagonia during mediaeval time. *Nature,* **369,** 546–549.

Trenberth, K. E., 1990: Recent observed interdecadal climate changes in the Northern Hemisphere. *Bull. Amer. Meteor. Soc.,* **71,** 988–993.

Wahl, K. L., 1992: Evaluation of trends in runoff in the western United States: Managing water resources during global change. *Proc. American Water Resources Association 28th Annual Conf. and Symp.,* Reno, NV, Amer. Water. Resour. Assoc., 701–710.

Wallace, J. M., and D. S. Gutzler, 1981: Teleconnections in the geopotential height field during Northern Hemisphere winter. *Mon. Wea. Rev.,* **109,** 784–812.

Webb, R. H., and J. L. Betancourt, 1990: Climatic variability and flood frequency of the Santa Cruz River, Pima County, Arizona. U.S. Geological Survey, Open-File Rep. 90-553, 69 pp. [Available from USGS, Federal Center, Box 25425, Denver, CO 80225.]

——, S. S. Smith, and V. A. S. McCord, 1991: *Historic Channel Change of Knab Creek, Southern Utah and Northern Arizona. Grand Canyon Natural History Association Monogr.,* No. 9, 90 pp. [Available from R. H. Webb, U.S. Geological Survey, 165 West Anklam Road, Tucson, AZ 85721.]

White, W. B., J. Lean, D. R. Cayan, and M. D. Dettinger, 1997. Response of global upper ocean temperature to solar irradiance anomalies. *J. Geophys. Res.,* **102,** 3255–3266.

Xu, J., 1993: The joint modes of the coupled atmospheric–ocean system observed from 1967 to 1986. *J. Climate,* **6,** 816–838.

Zhang, Y., J. M. Wallace, and D. S. Battisti, 1997: ENSO-like interdecadal variability: 1900–93. *J. Climate,* **10,** 1004–1020.